Topological characterization and early detection of bifurcations and chaos in complex systems using persistent homology

Khushboo Mittal, and Shalabh Gupta

Citation: Chaos **27**, 051102 (2017); doi: 10.1063/1.4983840
View online: https://doi.org/10.1063/1.4983840
View Table of Contents: http://aip.scitation.org/toc/cha/27/5
Published by the American Institute of Physics

Topological characterization and early detection of bifurcations and chaos in complex systems using persistent homology

Khushboo Mittal and Shalabh Gupta
Electrical and Computer Engineering, University of Connecticut, Storrs, Connecticut 06269, USA

(Received 11 April 2017; accepted 9 May 2017; published online 19 May 2017)

Early detection of bifurcations and chaos and understanding their topological characteristics are essential for safe and reliable operation of various electrical, chemical, physical, and industrial processes. However, the presence of non-linearity and high-dimensionality in system behavior makes this analysis a challenging task. The existing methods for dynamical system analysis provide useful tools for anomaly detection (e.g., Bendixson-Dulac and Poincare-Bendixson criteria can detect the presence of limit cycles); however, they do not provide a detailed topological understanding about system evolution during bifurcations and chaos, such as the changes in the number of subcycles and their positions, lifetimes, and sizes. This paper addresses this research gap by using topological data analysis as a tool to study system evolution and develop a mathematical framework for detecting the topological changes in the underlying system using persistent homology. Using the proposed technique, topological features (e.g., number of relevant k-dimensional holes, etc.) are extracted from nonlinear time series data which are useful for deeper analysis of the system behavior and early detection of bifurcations and chaos. When applied to a Logistic map, a Duffing oscillator, and a real life Op-amp based Jerk circuit, these features are shown to accurately characterize the system dynamics and detect the onset of chaos. *Published by AIP Publishing.*
[http://dx.doi.org/10.1063/1.4983840]

Complex dynamical systems often undergo critical transitions such as bifurcations and chaos due to parametric or nonparametric changes in the system. These transitions can lead to system anomalies, undesirable performance, and failures. Thus, early detection of these transitions and understanding their topological characteristics are essential for reliable operation of these systems. However, the presence of high-dimensionality and uncertainty makes analysis of these systems a challenging task. The existing model-based and data-driven methods for dynamical system analysis provide useful tools for anomaly detection; however, the features extracted by these methods do not provide detailed topological understanding to distinguish between the system behaviors before and after the critical transitions, such as changes in the number of subcycles and their positions, lifetimes, and sizes. This work addresses this gap and presents an innovative approach for dynamical system analysis using persistent homology. The proposed methodology extracts crucial topological features to gain deeper insights into system behavior for early detection of bifurcations and chaos. The methods proposed herein are applicable for broader applications in non-linear time series analysis, behavior prediction, and anomaly detection.

I. INTRODUCTION

"Complexity" in dynamical systems occurs due to several factors such as nonlinearity, high-dimensionality, time-varying operating conditions, and environmental uncertainties. Furthermore, complexity can become acutely conspicuous when parametric or nonparametric changes in the system lead to the evolution of behavioral patterns, causing critical transitions such as bifurcations and chaos. These transitions are usually characterized by changes in topological features (e.g., number, positions, and sizes of cycles and subcycles) of the system. These underlying changes can lead to system anomalies, undesirable performance, and failures. Thus, for safe and reliable operation of these systems, it is important to detect the critical transitions early by obtaining deeper insights into the topological changes in the system behavior. This topological information enables the system operator to take appropriate proactive actions for preventing bifurcations and chaos and maintaining the desired performance.

In recent decades, several model-based and data-driven approaches have been proposed for complex system analysis. Model based approaches include popular analytical methods such as the Bendixson-Dulac criterion and Poincare-Bendixson[14] criterion, which are able to predict the presence of limit cycles, but these methods are restricted to 2-D systems and cannot be extended to higher dimensions. Moreover, these methods do not provide topological information such as the presence of subcycles and their positions and sizes. Other analytical methods such as Harmonic Balance and Describing Functions[17] can provide an approximate estimate of the size of limit cycles, but they fail in systems revealing higher harmonics of nonlinearity. On the other hand, several data-driven methods have been developed such as recurrence plots,[16] correlation sum analysis,[8] Lyapunov exponents,[20] permutation entropy,[1] and symbolic dynamics.[9,10,12] These methods provide useful tools for anomaly detection when combined with statistical classification and prediction techniques; however, the features extracted using

TABLE I. Literature review of the existing methods for dynamical system analysis.

Existing methods	Main features	Limitations	Research gaps
Bendixson-Dulac criterion and Poincare-Bendixson[14] criterion	Detect the presence of limit cycles	Not applicable for high-dimensional systems ($D > 2$)	Existing methods do not provide topological information about the system behavior such as the presence of subcycles and their positions and sizes. This information is crucial as it could provide deeper insights into the system behavior as well as aid in early detection of bifurcation and chaos
Harmonic Balance and Describing Functions[17]	Provide an approximate estimate of the size of limit cycles	Linearization might not work for systems with higher harmonics of nonlinearity	
Data-driven methods such as recurrence plots,[16] correlation sum analysis,[8] Lyapunov exponents,[20] permutation entropy,[1] and symbolic dynamics[9,10,12]	Detection of anomalies or changes in system behavior	Do not provide a topological understanding to distinguish between the system behaviors before and after these transitions	

these methods do not provide any topological understanding to distinguish between the system behaviors before and after such transitions. Table I summarizes the limitations and the research gaps of these methods. In contrast, topological data analysis methods enable the extraction of features that can provide useful information about evolution of system behavior. In recent literature studies,[6] such features were used for the reconstruction of system dynamics. This paper, thus, presents a mathematical framework of topological data analysis for early detection of bifurcations and chaos as well as for understanding their topological characteristics.

In particular, this work utilizes persistent homology[5] based techniques for dynamical system analysis. Persistent homology provides a robust and accurate analysis of a dynamical system as it studies the system topology at different spatial resolutions. This leads to the persistence of only the major features of the underlying system and removes spurious effects of noise. Using this technique, different topological features such as the number of relevant k-dimensional holes and their positions, lifetimes, and sizes will be extracted to track the changes in the system topology. Here, the term *hole* refers to the enclosed regions formed in the phase diagram of system trajectories. These features provide important information about system behavior, e.g., the number of relevant 1-D holes increases with the increase in the number of subcycles.

The proposed solution is tested on three different dynamical systems. First, on the Duffing oscillator, it was able to determine the number of subcycles present in the system and timely detected the presence of chaos. Second, on the Logistic map, it captured the period doubling along with the onset of chaos. Finally, on the Op-amp based Jerk circuit it was again able to track the period-doubling cascades and the onset of chaos.

The key advantages of this approach are listed below:

- Extraction of features such as the number of relevant k-dimensional holes and their positions, sizes, and lifetimes that contain information about the system topology.
- Early detection of bifurcations and chaos by tracking the evolution of the above features.
- Robustness to noise and uncertainties and applicability on high-dimensional data.

II. TOPOLOGICAL DATA ANALYSIS

A. Simplicial complex and homology groups

The proposed features are obtained by applying persistent homology on simplicial complexes[18] that are constructed from the time series data generated from a dynamical system.[15] The construction of a simplicial complex from data is described below.

Simplicial Complex: A k-simplex is defined as a k-dimensional polytope which is a convex hull of its $k+1$ vertices. Fig. 1 illustrates some low-dimensional k-simplices for $0 \le k \le 3$: *vertices*, *edges*, *triangles*, and *tetrahedra*, respectively. A simplicial complex $\mathcal{R}$ is a set of simplices such that: (i) any face of a simplex from $\mathcal{R}$ is also in $\mathcal{R}$, (ii) the intersection of any two simplices $\sigma_1, \sigma_2 \in \mathcal{R}$ is either Ø or a face of both σ_1 and σ_2. It can be seen as a coarse approximation of the topological space in which the level of details is controlled by the scaling parameter ϵ. In this work, Vietoris-Rips (VR) and Witness complexes have been used for the construction of a simplicial complex from the time series data. In VR complex ($\mathcal{R}_\epsilon$), a k-simplex is added only when the pairwise intersection of all the points is less than the threshold ϵ. Fig. 2 demonstrates examples of some VR complexes constructed from point cloud data for different ϵ values. For $\epsilon = 0.4$, the complex has six 0-simplices. A 1-simplex is formed when ϵ is increased to 0.5. The number of 1-simplices keeps on increasing as the ϵ value is further increased, and for $\epsilon = 0.8$, two 2-simplices appear. For larger datasets, the exponential increase in the numbers of simplices would make the construction of the VR complex computationally inefficient. This problem can be addressed by using the *Witness*[2] complex, which is a more efficient simplicial complex built over a subset (known as *landmark* points) of the original time series data.

Next, homology groups are computed from these complexes to obtain information about the k-dimensional holes

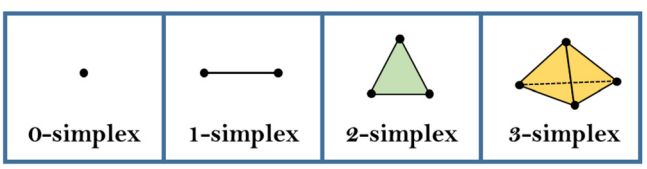

FIG. 1. Low-dimensional k-simplices for $0 \le k \le 3$.

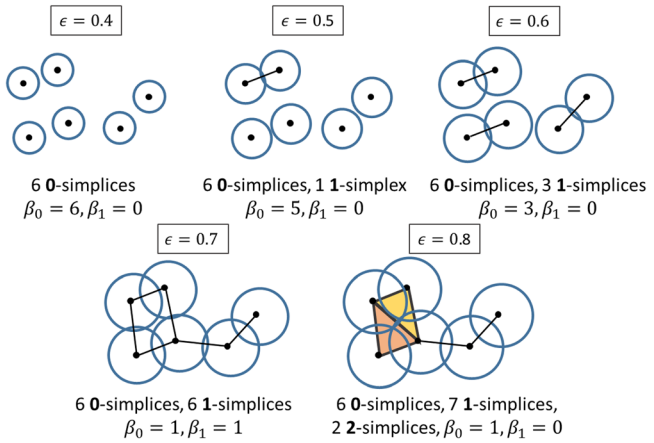

FIG. 2. Example of Vietoris-Rips complexes and corresponding Betti numbers for different scale parameters ϵ.

in topological space $\mathbb{X}$ in the form of the kth Betti number[5] (β_k). For mathematical details about the computation of these Betti numbers and homology groups, the readers are requested to see Appendix or refer to Refs. 7 and 24. Betti numbers capture the connectivity information of a space, and the physical meaning of these numbers is provided in Table II. Specifically, β_0 or the number of 0-dimensional holes refers to the number of connected components or clusters present in a space, and the number of 1-D holes or β_1 represents the number of enclosed regions or circular holes in space. For example, the 3-D torus shown in Fig. 3 has one connected component ($\beta_0 = 1$), two circular holes ($\beta_1 = 2$), and one void ($\beta_2 = 1$). Further examples of VR complexes and the corresponding Betti numbers are provided in Fig. 2.

B. Persistent homology

One of the limitations of these homology groups is that the topological information provided by them might not be optimal as it depends on the choice of scaling parameter ϵ used for their construction. A sufficiently small ϵ leads to a VR complex containing discrete data points; whereas for a sufficiently large ϵ, the complex would be a high-dimensional simplex. To overcome this limitation, persistent homology constructs these complexes for a range of ϵ values instead of creating only one simplicial complex for a random ϵ value. The idea of persistence focuses on examining the homology of these iterated complexes (called as *filtration*), rather than the homology of the individual complexes $\mathcal{R}_\epsilon$, thus revealing the persisting features and filtering out noise and other artefacts. The resulting persistent homology groups[5] provide information of each k-dimensional hole (or

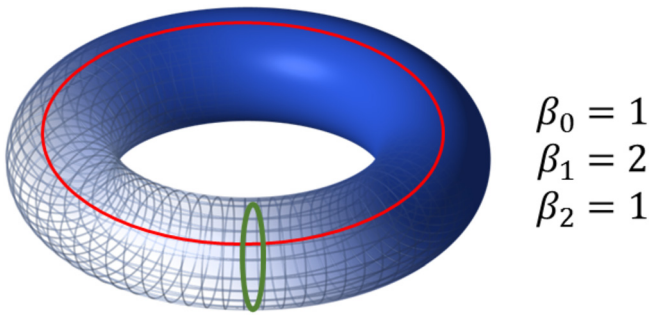

FIG. 3. Betti numbers for a 3-D torus.

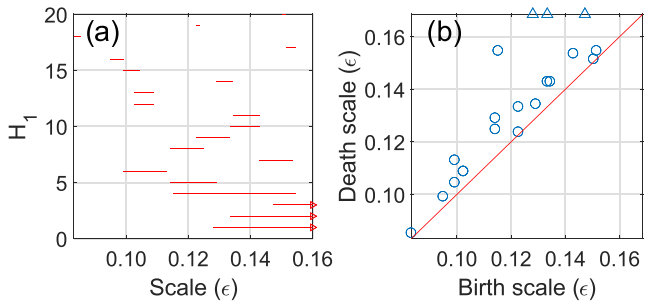

FIG. 4. Illustration of persistent homology features: (a) barcode plot for 1-D holes and (b) persistence diagram.

homology group generator), which can be represented by a multiset of points, Δ_k as defined below

$$\Delta_k = \{(u, v) \in \mathbb{R}^2 : u, v \geq 0, u \leq v\}, \tag{1}$$

where u and v represent the birth and death scales of a hole, respectively. The evolution of these holes (increase and decrease in Betti numbers) over the course of filtration is represented by *persistent intervals*. The most persistent or the longest intervals represent the true Betti numbers of a topological space.

These intervals are visualized using *barcode plots*[7] shown in Fig. 4(a), which are obtained from a filtration constructed from point cloud data. These plots are a graphical representation of the persistent homology groups, where the horizontal axis corresponds to the scale ϵ and the vertical axis represents the holes (or homology group generators). Each interval in this plot summarizes the lifetime of a hole, clearly indicating its birth and death scales. Persistence diagrams for the same data are shown in Fig. 4(b). The intervals in the barcode plot are represented as points in the persistence diagram, and the points far above the diagonal correspond to the longer persistent intervals. Longer intervals are the prominent ones defining the underlying system topology.

TABLE II. Physical interpretation of Betti numbers.

(β_k)/k-D Holes	1-D	2-D	3-D
β_0(0–D Holes)	No. of connected components	No. of connected components	No. of connected components
β_1(1–D Holes)	0	No. of circular holes	No. of circular holes
β_2(2–D Holes)	0	0	No. of voids
β_n(n–D Holes) for $n > 2$	0	0	0

Shorter persisting intervals can occur because of the presence of noise or artefacts in the data and are thus ignored.

III. PROPOSED TOPOLOGICAL FEATURES

Since persistent intervals capture the true Betti numbers of a space, topological features derived from these intervals are used for dynamical system analysis in this paper. These features are described below:

(1) **Number of relevant *k*-D holes[19] ($\mathbf{nrel}_k$) for $k \geq 0$**: Given persistent homology information where each hole i has a birth time u_i and death time v_i, the lifetime of a hole is defined as

$$\mathrm{L}_i = v_i - u_i. \tag{2}$$

The maximum lifetime of k-D holes, ML_k, is

$$\mathrm{ML}_k = \max_{1 \leq i \leq |\Delta_k|} L_i, \tag{3}$$

where Δ_k is defined in Eq. (1). Then, nrel_k is computed as the number of holes whose lifetime is greater than $\theta * \mathrm{ML}_k$, where $\theta \in (0, 1)$. This feature corresponds to the number of the longest persistent k-dimensional holes in topological space $\mathbb{X}$. For the 3-D torus shown in Fig. 3, $\mathrm{nrel}_0 = 1$, $\mathrm{nrel}_1 = 2$, $\mathrm{nrel}_2 = 1$, and $\mathrm{nrel}_k = 0$ for $k > 2$.

(2) **Average lifetime of *k*-D holes[19] ($\mathbf{avg}_k$)**: The average lifetime of all the k-D holes is obtained as

$$\mathrm{avg}_k = \frac{1}{|\Delta_k|} \Sigma_{i=1}^{|\Delta_k|} L_i. \tag{4}$$

(3) **Expected orbit period (K_{orbit})**: In a period-doubling cascade, the period K_{orbit} of the periodic orbit keeps on doubling until the system manifests into chaos. As this period increases, more stable solutions appear, which can be seen as different clusters in delay embedding plots as shown in Fig. 6(b). An estimate of this period can be obtained using the number of simplices present in a filtration. The number of simplices varies proportionally with the orbit period and becomes half when the period is doubled as the data points get divided among new solutions/clusters. If the total number of simplices for a system is S, then K_{orbit} is estimated as

$$K_{\mathrm{orbit}} = \left\lfloor \frac{S_1}{S} \right\rfloor, \tag{5}$$

where the operator $\lfloor * \rfloor$ refers to the floor operation and the constant S_1 refers to the number of simplices obtained for a stable system with ideal parameter values and period-1 orbits converging to 1 fixed point.

(4) **Diameter of a hole ($\mathbf{D_i}$)**: Using persistent homology, we can obtain all the data points/vertices belonging to a hole. If a hole i contains N vertices, then its diameter, D_i, is computed as follows:

$$\mathrm{D}_i = \max_{1 \leq p,q \leq N} \|\mathbf{x_p} - \mathbf{x_q}\|, \tag{6}$$

where the operator $\|*\|$ refers to the l^2-norm or Euclidean distance between the vertices $\mathbf{x_p} \in \mathbb{R}^M$ and $\mathbf{x_q} \in \mathbb{R}^M$, belonging to the hole. In addition to D_i, the sum ($\Sigma_{i=1}^{|\Delta_k|} D_i$) and average of diameters of all k-D holes can also serve as useful topological features.

(5) **Maximum diameter of *k*-D holes ($\mathbf{maxD}_k$)**: Given the diameters D_i of all k-dimensional holes, the maximum diameter, maxD_k, is defined as

$$\mathrm{maxD}_k = \max_{1 \leq i \leq |\Delta_k|} D_i. \tag{7}$$

Here, maxD_k corresponds to the size of the largest or the most prominent hole.

(6) **Maximum Distance between *k*-D holes ($\mathbf{maxDist}_k$)**: For a k-D hole i in M-dimensional space containing N vertices, the hole center, $\mathbf{xc_i} = (\mathrm{xc}_i^1, \mathrm{xc}_i^2, \ldots \mathrm{xc}_i^M)$, can be computed as

$$\mathrm{xc}_i^m = \frac{1}{N} \Sigma_{j=1}^{N} \mathrm{x}_j^m \quad \text{for } m = 1, 2, \ldots M, \tag{8}$$

where $\mathbf{x_j} \in \mathbb{R}^M$ is a vertex belonging to the hole. The distance between two holes i and j is then defined as

$$\mathrm{dist}_k^{ij} = \|\mathbf{xc_i} - \mathbf{xc_j}\|. \tag{9}$$

The maximum distance between all the k-D holes can be obtained as

$$\mathrm{maxDist}_k = \max_{1 \leq i,j \leq |\Delta_k|} \mathrm{dist}_k^{ij}. \tag{10}$$

The choice of the topological features used for dynamical system analysis depends on the specific transitions exhibited by that system. A training process is required to choose the relevant features, the range of scale parameters ϵ, and the parameters θ and S_1 in order to apply the proposed technique on a dynamical system.

IV. RESULTS

The performance of this algorithm is studied on three different dynamical systems:

(1) Duffing oscillator which is a continuous time system that exhibits period-3, period-5, and period-4 cycles followed by chaotic behavior.
(2) Logistic map which is a discrete time system that exhibits period-doubling cascades followed by chaotic behavior.
(3) Op-amp based Jerk circuit which is a real life continuous time system that exhibits period-doubling cascades followed by chaotic behavior.

Comparison results with three existing dynamical system analysis methods: Largest Lyapunov exponent,[20] permutation entropy,[1] and correlation dimension[8] are also presented to highlight the advantages of the proposed method. All the persistent homology calculations are done in Matlab using the computational topology toolbox **Javaplex.**[22] The maximum computation time for the proposed features is less than four

minutes for all the three systems, which is much faster than the timescale of evolution of system parameters. The detailed analysis including system simulations, feature extraction, test times, and comparison results are as follows:

(1) **Duffing oscillator**: The non-autonomous forced Duffing system[13] is modeled as

$$\ddot{y} + \delta\dot{y} + \alpha y(t) + \beta y^3(t) = \gamma\cos(\omega t). \tag{11}$$

The system behavior is studied for a range of driving force amplitudes (γ) by keeping the other parameters constant. It is simulated for $\gamma \in [0.35, 0.38]$, $\beta = 1$, $\alpha = 1$, $\delta = 0.3$, and $\omega = 1.2$ with initial conditions $y(0) = 0$ and $\dot{y}(0) = 0$. An additive white Gaussian noise (AWGN) of 30 dB signal-to-noise ratio (SNR) is added to this system which is denoised using wavelet filtering.[3,4] The phase portrait plots for different γ values are shown in Fig. 5(a). The system exhibits period-3 oscillations with 3 subcycles at $\gamma = 0.36$, which change to 5 subcycles (period-5) at $\gamma = 0.362$ and further to 4 subcycles (period-4) at $\gamma = 0.375$. A sudden change in the system behavior is observed at $\gamma = 0.38$, which occurs due to the end of period-4 behavior which is followed by a transition region until $\gamma = 0.382$ after which the system exhibits the chaotic phenomenon. The transition region between the period-4 behavior and the chaos is marked by dotted lines in the analysis plots in Fig. 5.

Persistent homology is applied on the filtration of the Witness complex with 500 landmark points constructed over these simulated data for scale parameter ϵ in the range of [0, 0.001] for different values of γ. The three features, nrel_1 with $\theta = 0.7$, average lifetime of 1-D holes (avg_1), and diameter of 1–D holes (D_i), are extracted from the persistent homology groups with an average computation time of 29 s. As seen in Figs. 5(b-i) and 5(b-ii), nrel_1 and avg_1 accurately track the changes in the number of subcycles for period-3, period-5 and period-4 oscillations, clearly detecting the system evolution before the onset of chaos. The variations in diameters of the 5 holes are shown in Fig. 5(b-iii). Out of the 5 holes, the diameters of holes 3 and 4, D_3 and D_4, are able to accurately track the changes in γ values much before the change in the subharmonic period and the onset of chaos, thus providing early detection of the transitions. Figs. 5(c-i)–5(c-iii) illustrate the performance of the features obtained using the Lyapunov exponent,

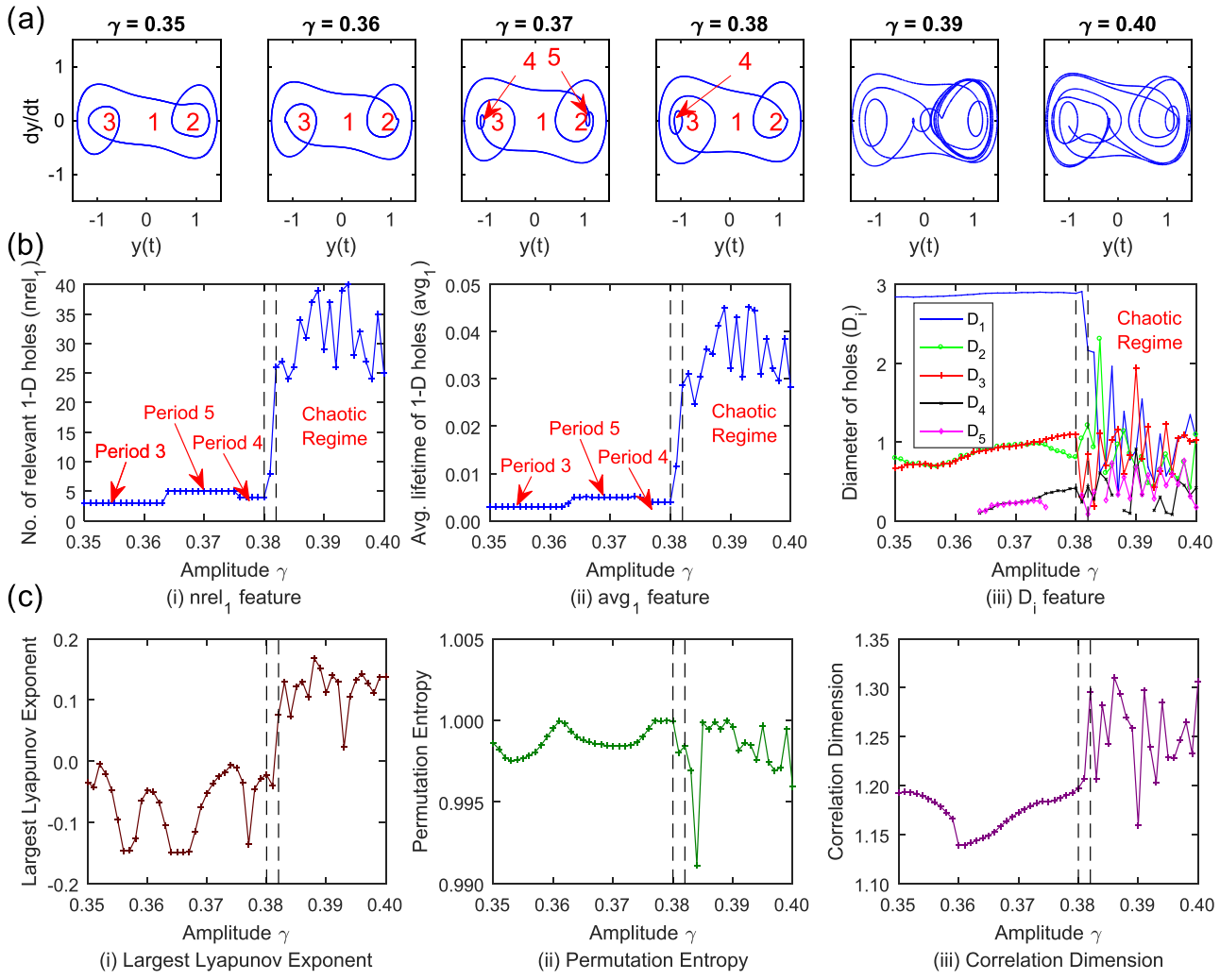

FIG. 5. Analysis of the Duffing oscillator: (a) phase portrait plots for different γ values, (b) proposed topological features, and (c) comparison results with the existing methods.

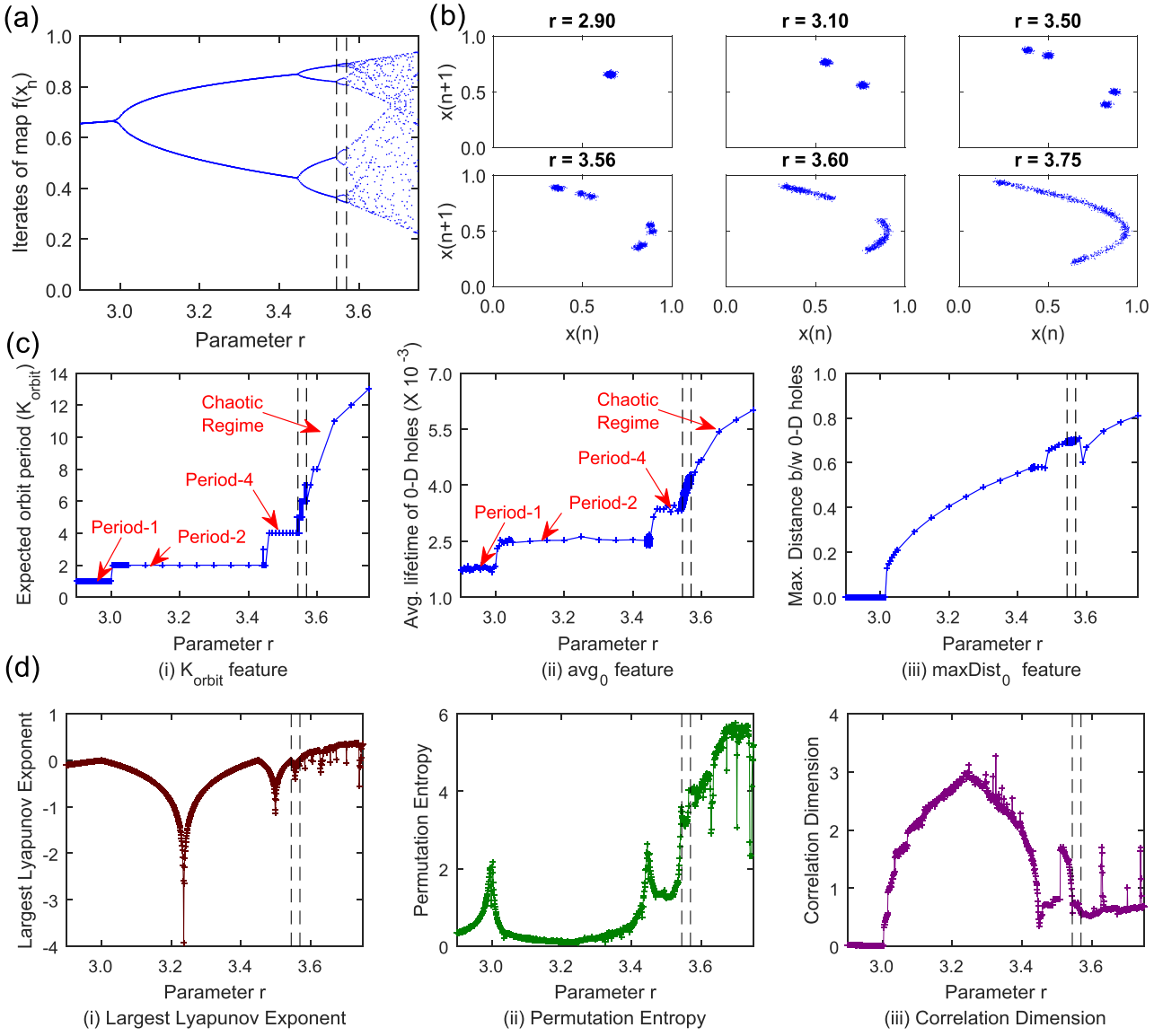

FIG. 6. Analysis of the Logistic map: (a) period-doubling cascade, (b) phase space reconstruction plots for different r values, (c) proposed topological features, and (d) comparison results with the existing methods.

permutation entropy, and correlation dimension methods, respectively, for this system. While all these methods are able to detect the onset of chaos and bifurcation points, they fail to provide a clear trend for the early detection of these changes. Moreover, none of these existing methods provide any deeper insights into the topological characteristics of the system such as the number and sizes of subcycles.

(2) **Logistic map**: It is a discrete-time demographic model showing the evolution of the population size as a function of the growth rate

$$x_{n+1} = rx_n(1 - x_n), \tag{12}$$

where $x_n \in [0, 1]$ represents the ratio of the existing population to the maximum possible population and r is the growth rate. The Logistic map is simulated for $r \in [2.5, 3.75]$, and AWGN with 30 dB SNR is added to these data for realistic simulations. Fig. 6(a) shows the variation in the steady state population with growth rate r. The system enters into a period-doubling bifurcation with period-2 at $r = 3$ and period-4 at $r = 3.45$. The period-4 behavior ends at $r = 3.544$ after which the system undergoes further rapid period-doublings before entering into chaos at $r = 3.569$. The transition region highlighting the end of the period-4 regime and the onset of the chaotic regime is marked by dotted lines in the analysis plots in Fig. 6.

Phase space reconstruction using Takens' theorem[21] (delay = 1 and embedding dimension = 2) is applied on the time series data, and the stable solutions are represented as different clusters in Fig. 6(b). Persistent homology is applied on the VR complex filtration constructed from these delay embedded data over the scale range of [0, 0.01] for different r values, and K_{orbit}, avg_0, and maxDist_0 features are extracted with an average computation time of 3 s. For computing K_{orbit}, S_1 is set as the number of simplices obtained for $r = 2.9$ when the system has 1 fixed point. Figs. 6(c-i) and 6(c-ii) show the

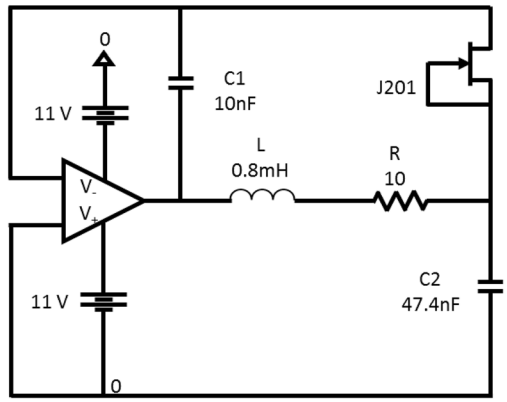

FIG. 7. Schematic of the Jerk circuit.[23]

variation in K_{orbit} and avg_0 with parameter r, respectively. Both the features are able to detect the period-doubling bifurcations and the onset of chaos. The K_{orbit} feature also shows the exact period of the period-doubling cascade. The $maxDist_0$ feature shown in Fig. 6(c-iii) enables early detection of the bifurcations and chaos. The features obtained with other existing features are shown in Fig. 6(d). While all these three methods, Lyapunov exponent, permutation entropy and correlation dimension, as shown in Figs. 6(d-i)–6(d-iii), respectively, are able to detect critical transition points in the system, they do not show any clear trend with respect to the changes in the bifurcation parameter. Moreover, none of these methods provide any topological understanding about the system behavior. In comparison, the proposed topological features are able to timely detect the critical changes, provide information about system behavior, and also perform early detection of bifurcations and chaos.

(3) **Jerk circuit**: It is a single op-amp based five-component Jerk circuit[23] which experiences the period-doubling cascade and chaotic phenomenon. A schematic representation of this circuit is shown in Fig. 7. This non-linear dynamical system is modeled as a continuous time system as opposed to the previously discussed Logistic map. It is described using a three-dimensional state vector $F = [x, y, z]^T$ as follows:

$$\frac{dF}{dt} = \begin{bmatrix} 0 & 0 & 0 \\ 0 & 0 & -\alpha \\ -\beta & \beta & -\beta\gamma \end{bmatrix} F + \begin{bmatrix} 1 \\ \alpha \\ 0 \end{bmatrix} \varphi(y), \tag{13}$$

where α, β, and γ are three system parameters and φ is a piecewise nonlinear function defined as

$$\varphi(y) = \begin{cases} -y & \text{if } y \le 1 \\ -1 & \text{if } y > 1. \end{cases} \tag{14}$$

It is studied for a range of parameters $\gamma \in [0.16, 0.11]$ by keeping the other two parameters constant at $\alpha = 0.025$ and $\beta = 0.765$. It is simulated with initial conditions such as $x(0) = 0.1$, $y(0) = -5 \times 10^{-7}$, and $z(0) = -1$, and AWGN with 30 dB SNR is added to the system. The simulation data are denoised using wavelet filtering,[3,4] and the phase portrait plots for different γ values are shown in Fig. 8(b). The system shows period-1 (1 subcycle), period-2 (2 subcycles), and period-4 (4 subcycles) oscillations for $\gamma = 0.16$, $\gamma = 0.137$, and $\gamma = 0.123$, respectively. It enters into chaos on further decreasing the γ value at $\gamma = 0.119$. The transition region into the chaotic regime after the end of period-4 behavior is shown by dotted vertical lines in Fig. 8, highlighting the control parameters at which these changes occur. The complete bifurcation diagram describing the variation in the maximum value of y values as a function of parameter γ is shown in Fig. 8(a).

Persistent homology is applied on the filtration of the Witness complex with 1000 landmark points constructed over the two-dimensional time series data $[x, y]^T$ for scale parameter $\epsilon \in [0, 1]$ with an average computation time of 220 s. Then topological features including $nrel_1$ with $\theta = 0.4$, avg_1, and maximum diameter of 1-D holes, $maxD_1$, are extracted from the persistent homology groups. As shown in Figs. 8(c-i) and 8(c-ii), $nrel_1$ and avg_1 features are able to track system evolution by detecting the changes in the period of the period-doubling bifurcation and the onset of chaos. These features can clearly identify the period-1, period-2, and period-4 regimes and detect the chaotic behavior. Early detection of bifurcations and chaos is performed with the $maxD_1$ feature as shown in Fig. 8(c-iii). The analysis of this system using other existing methods is also done to compare the performance of the proposed method, and the resulting features are shown in Fig. 8(d). The Lyapunov exponent method, shown in Fig. 8(d-i), is able to detect the onset of chaos but does not track the system evolution very well. Permutation entropy (Fig. 8(d-ii)) and correlation dimension (Fig. 8(d-iii)) methods are able to track system evolution and do early detection but do not provide any topological understanding about the system behavior. The proposed topological features provide this understanding and are able to track system behavior along with the onset of chaos and provide early indication of these critical transitions.

V. CONCLUSIONS AND FUTURE WORK

To conclude, this work provides an innovative approach for topological characterization and early detection of bifurcations and chaos in a dynamical system in an automated manner. While analysis of nonlinear dynamical systems is not a straightforward task, the proposed method, based on persistent homology, is successful in the early detection of critical transitions. On the Duffing oscillator, the extracted topological features (such as the number of relevant k-D holes and their positions, sizes, and lifetimes) have been demonstrated to detect the number of subcycles and chaotic behavior. On the Logistic map and the Jerk circuit, they are shown to detect period-doubling bifurcations and the onset of chaos. Comparison results with other existing methods in the literature are also provided to highlight the advantages of our approach. These results illustrate that the proposed method is able to address the research gaps in the literature by extracting features which provide crucial topological information about the system behavior. In the future, we would like to further develop and generalize the

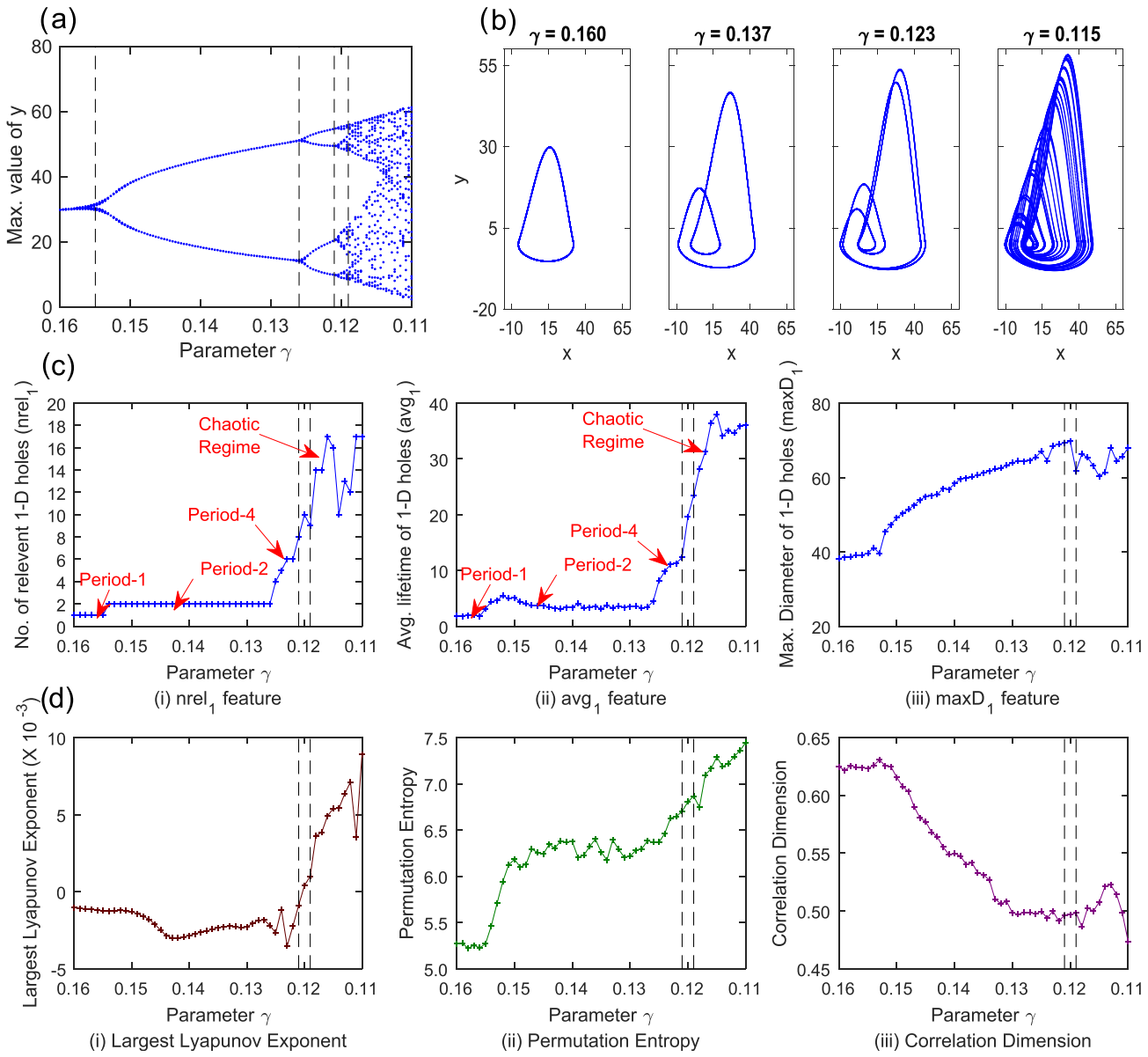

FIG. 8. Analysis of the Jerk circuit: (a) period-doubling cascade, (b) phase portrait plots for different γ values, (c) proposed topological features, and (d) comparison results with the existing methods.

proposed topological features for anomaly detection in other real world time series data, for example, epileptic seizure detection, behavior prediction and fault detection.

APPENDIX: CHAIN COMPLEX AND HOMOLOGY GROUPS

Witness Complex:[2] The Vietoris-Rips complexes are often difficult in handling because of the exponential increase in their size with an increase in the number of points. This issue can be handled by building the Witness complex on a subset, $Q \subset P$ of point cloud data P, instead of using all the points. The subset Q is known as *landmark*[2] points. These landmark points can be obtained using either of the two methods: *maxmin* and *random*. Witness complexes are of two types:

(1) Weak Witness Complex: A simplex $\sigma = \{q_1,q_2,\ldots,q_n\}$ is weakly witnessed by $x \in P$ if $d(q, x) \leq d(p, x)$ for every $q \in \{q_1, q_2,\ldots,q_k\}$ and $p \in Q\backslash\{q_1, q_2, \ldots, q_k\}$.

(2) Strong Witness Complex: Additionally, the complex is a *strong* witness complex if $d(q_1, x) = \cdots = d(q_k, x)$.

Chain Complex: Given a simplicial complex $\mathcal{R}$, a k-chain $c \in C_k$ is a linear combination of k-simplices and is defined as $c = \sum_i n_i[\sigma_i]$, where $\sigma_i \in \mathcal{R}$ and coefficients $n_i \in \mathbb{Z}$. The group of k-chains in $\mathcal{R}$ is defined as the free Abelian group on the set of oriented k-simplices in $\mathcal{R}$ and is denoted by C_k. For a simplex $\sigma = [v_0, v_1,\ldots v_k] \in c$, the boundary operator $\partial_k : C_k \to C_{k-1}$ is a linear operator and is defined as

$$\partial_k \sigma = \sum_i (-1)^i [v_0, v_1, \ldots, \hat{v}_i, \ldots, v_k], \tag{A1}$$

where $\hat{v}_i$ denotes the deleted vertex. Because of linearity, this operator can be defined over the entire chain space. It is easy to show that the boundary of a boundary is always empty, i.e., $\partial_k \partial_{k+1} = 0$, thus implying $Image(\partial_{k+1}) \subseteq Kernel(\partial_k)$.

Homology Groups:[7,24] Using the subgroups, Image(∂_{k+1}), and Kernel(∂_k), the kth *homology* group H_k of $\mathcal{R}$ is defined as the quotient group

$$H_k(\mathcal{R}) = Kernel(\partial_k)/Image(\partial_{k+1}). \tag{A2}$$

Homology can be seen as a set of topological invariants of space $\mathbb{X}$ represented by *homology groups*[11] $H_0(\mathbb{X})$, $H_1(\mathbb{X}), \ldots, H_k(\mathbb{X})$.

Betti Numbers: The kth homology group H_k provides information about the k-dimensional holes in $\mathbb{X}$ and is represented by the kth Betti number, which is the rank of the k-th homology group

$$\beta_k = \text{rank}(H_k). \tag{A3}$$

A sequence of simplicial complexes forms a filtration, $R = (\mathcal{R}_i)_1^N$, for an increasing sequence of parameter values $(\epsilon_i)_1^N$, comprised of the inclusion maps with the following ordering:

$$\emptyset = \mathcal{R}_0 \overset{\iota}{\hookrightarrow} \mathcal{R}_1 \overset{\iota}{\hookrightarrow} \mathcal{R}_2 \overset{\iota}{\hookrightarrow} \ldots \overset{\iota}{\hookrightarrow} \mathcal{R}_{N-1} \overset{\iota}{\hookrightarrow} \mathcal{R}_N. \tag{A4}$$

Because of linearity, the chain complexes are comprised of similar inclusion maps or chain maps $f_*^i : C_*^i \to C_*^{i+1}$. Persistent homology is then defined using these chain maps as follows.

Persistent Homology:[24] For $1 \le i < j \le N$, the persistent homology group $H_*^{i \to j}(C)$ for a chain complex C is defined as the image of the homomorphism induced by the chain map $x_* : H_*(C_*^i) \to H_*(C_*^j)$.

[1]C. Bandt and B. Pompe, "Permutation entropy: A natural complexity measure for time series," Phys. Rev. Lett. **88**, 174102 (2002).
[2]V. De Silva and G. E. Carlsson, "Topological estimation using witness complexes," in *Eurographics Symposium on Point-Based Graphics* (SPBG) (2004), Vol. 4, pp. 157–166.
[3]D. L. Donoho, "De-noising by soft-thresholding," IEEE Trans. Inf. Theory **41**, 613–627 (1995).
[4]D. L. Donoho and J. M. Johnstone, "Ideal spatial adaptation by wavelet shrinkage," Biometrika **81**, 425–455 (1994).
[5]H. Edelsbrunner, D. Letscher, and A. Zomorodian, "Topological persistence and simplification," Discrete Comput. Geom. **28**, 511–533 (2002).
[6]J. Garland, E. Bradley, and J. D. Meiss, "Exploring the topology of dynamical reconstructions," Phys. D **334**, 49–59 (2016).
[7]R. Ghrist, "Barcodes: The persistent topology of data," Bull. Am. Math. Soc. **45**, 61–75 (2008).
[8]P. Grassberger and I. Procaccia, "Measuring the strangeness of strange attractors," in *The Theory of Chaotic Attractors* (Springer, 2004), pp. 170–189.
[9]S. Gupta and A. Ray, "Pattern identification using lattice spin systems: A thermodynamic formalism," Appl. Phys. Lett. **91**, 194105 (2007).
[10]S. Gupta and A. Ray, "Statistical mechanics of complex systems for pattern identification," J. Stat. Phys. **134**, 337–364 (2009).
[11]A. Hatcher, *Algebraic Topology* (Cambridge University Press, 2002).
[12]D. K. Jha, D. S. Singh, S. Gupta, and A. Ray, "Fractal analysis of crack initiation in polycrystalline alloys using surface interferometry," EPL (Europhys. Lett.) **98**, 44006 (2012).
[13]D. Jordan and P. Smith, *Nonlinear Ordinary Differential Equations: An Introduction for Scientists and Engineers* (Oxford University Press on Demand, 2007).
[14]H. K. Khalil and J. Grizzle, *Nonlinear Systems* (Prentice Hall, New Jersey, 1996), Vol. 3.
[15]S. Maletić, Y. Zhao, and M. Rajković, "Persistent topological features of dynamical systems," Chaos **26**, 053105 (2016).
[16]N. Marwan, M. C. Romano, M. Thiel, and J. Kurths, "Recurrence plots for the analysis of complex systems," Phys. Rep. **438**, 237–329 (2007).
[17]A. I. Mees, *Dynamics of Feedback Systems* (John Wiley & Sons, Inc., 1981).
[18]J. R. Munkres, *Elements of Algebraic Topology* (Addison-Wesley Menlo Park, 1984), Vol. 2.
[19]C. M. Pereira and R. F. de Mello, "Persistent homology for time series and spatial data clustering," Expert Syst. Appl. **42**, 6026–6038 (2015).
[20]T. D. Sauer, J. A. Tempkin, and J. A. Yorke, "Spurious lyapunov exponents in attractor reconstruction," Phys. Rev. Lett. **81**, 4341 (1998).
[21]F. Takens, "Detecting strange attractors in turbulence," in *Dynamical Systems and Turbulence, Warwick 1980* (Springer, 1981), pp. 366–381.
[22]A. Tausz, M. Vejdemo-Johansson, and H. Adams, "JavaPlex: A research software package for persistent (co)homology," in *Proceedings of ICMS 2014, Lecture Notes in Computer Science 8592*, edited by H. Hong and C. Yap (2014), pp. 129–136, see http://appliedtopology.github.io/javaplex/.
[23]R. Tchitnga, T. Nguazon, P. H. L. Fotso, and J. A. Gallas, "Chaos in a single op-amp–based jerk circuit: Experiments and simulations," IEEE Trans. Circuits Syst. **63**, 239–243 (2016).
[24]A. Zomorodian and G. Carlsson, "Computing persistent homology," Discrete Comput. Geom. **33**, 249–274 (2005).